Freescale Semiconductor
Application Note

Document Number: AN4247
Rev. 2, 07/2011

Layout Recommendations for PCBs Using a Magnetometer Sensor

by: Talat Ozyagcilar
Applications Engineer

Contents

1 Introduction

This application note is intended to guide engineers in the successful design of Printed Circuit Boards (PCBs) incorporating magnetometer sensors. For convenience, the application discussed is an electronic compass (or eCompass) designed into a smartphone but the guidelines are equally applicable to other products using a magnetometer.

This note covers:

- Characteristics of the geomagnetic field
- Sensing range and resolution required in the magnetometer
- Level of accuracy needed from the calibration software
- Physics of magnetic interference from hard and soft iron effects and PCB currents
- Guidelines for component selection
- Experimental approach to visualize field distortions prior to layout and fabrication of the PCB

The mathematical formalism of hard and soft iron interference is provided in the Mathematical Annex for engineers wishing to understand the theoretical derivation of ellipsoidal measurement loci.

Additional information on the mathematics of a tilt-compensated eCompass can be found in the Freescale Application Note AN4248 “Implementing a Tilt-Compensated eCompass using Accelerometer and Magnetometer Sensors”. This and other application notes can be downloaded from http://www.freescale.com.

1.1 Key Words

eCompass, Geomagnetic, Magnetometer, Hard Iron, Soft Iron, Layout, Calibration, Ferromagnetic.

1.2 Summary

- A smartphone magnetometer measures the sum of the geomagnetic field plus magnetic interference generated by ferromagnetic components on the smartphone PCB. This interference is classified into permanent hard iron and induced soft iron components.
- The magnitude of hard iron and soft iron interference can exceed 1000 μT and saturate the magnetometer if care is not taken to minimize the use of ferromagnetic components, such as speakers, and to optimize the PCB layout by placing the magnetometer away from sources of magnetic interference.
- Software calibration algorithms are required to calculate the characteristics of, and mathematically remove, both hard iron and soft iron interference from the magnetometer readings allowing the geomagnetic field component to be measured with an error below 0.5 μT.
- An experimental approach is described which uses a Freescale RD4247MAG3110 eCompass evaluation board to measure and visualize the level of hard iron and soft iron interference prior to PCB fabrication.

2 The Geomagnetic Field

The magnitude of the earth's magnetic field (the geomagnetic field) varies over the surface of the earth from a minimum of 22 μT over South America to a maximum of 67 μT south of Australia. The heading of an eCompass is determined from the relative strengths of the two horizontal geomagnetic field components and these vary from zero at the magnetic poles to a maximum of 42 μT over East Asia. Detailed geomagnetic field maps are available from the *World Data Center for Geomagnetism* at http://wdc.kugi.kyoto-u.ac.jp/igrf/.

A rough and ready estimate of the error in an eCompass heading is given in radians by the ratio of the error in geomagnetic field estimation to the horizontal geomagnetic field strength. For example, the lowest value of the horizontal field strength likely to be experienced by a smartphone user is 10 μT in northern Canada and Russia. A compass heading accuracy of 0.05 radians or 3 degrees therefore requires that the error in estimating the geomagnetic field be no more than 0.5 μT.

3 Magnetic Interference within the Smartphone

Unlike accelerometer, pressure, and gyroscope MEMS sensors, which use mechanical sensing elements unaffected by electromagnetic components on the PCB, magnetometers are sensitive to the magnetic fields generated by other circuit components.

The most common magnetic field sources are:

- permanent ferromagnets (as found in speakers or buzzers).
- induced fields within any ferromagnetic material lacking a permanent field (such as sheet steel).
- fields generated by current flows (ranging from strong currents in power supply tracks to smaller currents within coils).

Even in a well-designed smartphone, these sources create extraneous fields with magnitudes approaching 1000 μT in the vicinity of the magnetometer placing severe constraints on the performance of both the magnetometer and the calibration software running within the smartphone eCompass application. The magnetometer must have an operating range of ±1000 μT to accommodate the sum of the geomagnetic and interfering fields and the calibration software must identify and remove this interference to accuracy better than 0.5 μT or one part in two thousand for 1000 μT interference.

Designers should not assume that the calibration software will always correct for a poor layout. Component selection and layout should therefore be optimized to reduce the interfering fields as much as is realistically feasible. Smaller interference fields ease the job of the calibration software and result in more accurate compass headings.

4 Hard Iron Interference

'Hard iron' magnetic fields are those which are generated by permanently magnetized ferromagnetic components on the PCB, such as an audio speaker or buzzer. Permanently magnetized components also create induced magnetic fields in normally unmagnetized ferromagnetic materials in their vicinity. Since the magnetometer and all components on the PCB are in fixed positions with respect to each other, the hard iron interference manifests as an additive magnetic field vector when measured in the magnetometer reference frame.

It makes little sense for manufacturers to supply carefully calibrated zero field offset magnetometers into the smartphone market since the magnetometer will be exposed to an unknown additive hard iron field. The manufacturer will typically specify only the limits between which the zero field offset will lie. The magnetometer zero field offset is also independent of the smartphone orientation and therefore simply adds to the hard iron field. The calibration algorithm then adds the magnetometer zero field offset to the PCB hard iron interference and removes both.

Figure 1 shows the modelling of the distortion of the geomagnetic field by three permanent magnets creating hard iron interference. The first image shows the field of the permanent magnets in the absence of an external field. The second image shows the combined field of the permanent magnets and the external field.

A magnetometer located in the vicinity of the magnets will see the sum of the geomagnetic field and the hard iron field and will compute an erroneous compass heading in the absence of calibration software.

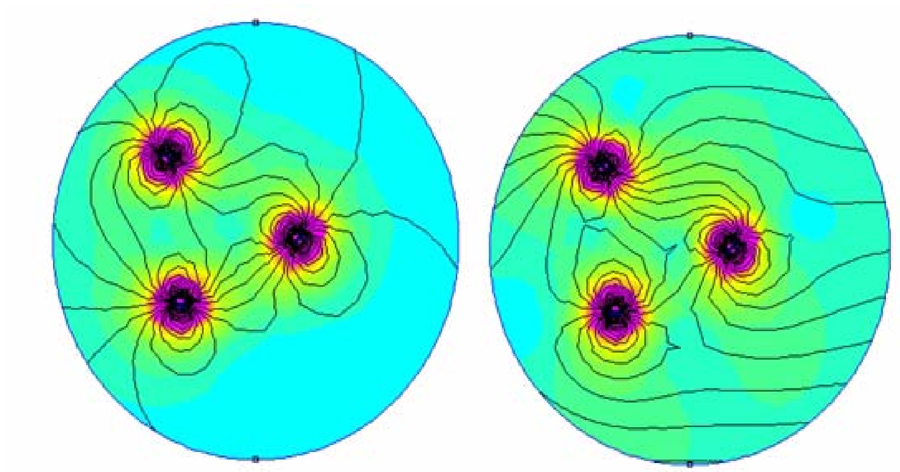

Figure 1. Hard iron disturbance of a uniform magnetic field

Hard iron interference can be minimized by a common sense strategy of avoiding, or selecting alternatives to, strongly magnetized ferromagnetic components and placing the magnetometer as far away as possible from such components.

5 Soft Iron Interference

'Soft iron' interference is created by the induction of a temporary magnetic field into normally unmagnetized ferromagnetic components, such as steel shields and batteries, on the PCB by the geomagnetic field.

Soft iron effects are more complex to model than hard iron since the induced field depends on the relative orientation of the geomagnetic field to the soft iron components. Earth's geomagnetic field is a fixed vector, however, its directional influence on the soft iron field varies and is dependent on the smartphone orientation. Soft iron effects induced by the geomagnetic field are therefore dependent on the smartphone orientation.

While the hard iron interfering field can be modelled as a simple additive three-component magnetic field vector, the soft iron interfering field manifests as axes with high magnetic permeability within the smartphone and is normally modelled as a six-component symmetric matrix.

Figure 2 illustrates the distortion of a uniform external magnetic field by three unmagnetized ferromagnetic bars oriented in different directions. The first image shows that there is no field in the absence of the external field. The second image shows the sum of the induced field in the bars and the external field. The bars become magnetized by the external field and steer it along their axes.

As shown in the hard iron field example, a magnetometer located in the midst of soft iron components will measure a magnetic field which may point in a very different direction to the geomagnetic field.

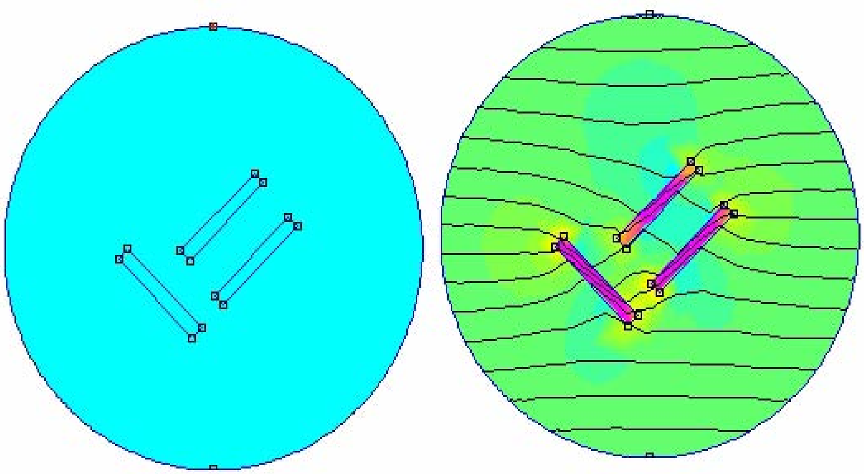

Figure 2. Soft iron disturbance of a uniform magnetic field

6 Fields from PCB Currents

Fixed currents, whether in PCB tracks or within coils, will generate fixed magnetic fields which add to the hard iron component. Calibration software will attempt to calibrate these fields and remove them, but it is good practice to minimize these fields. The strength of the resulting field measured at the magnetometer follows the standard rules of electromagnetism: the generated field is proportional to the current, is multiplied by coherent addition of the same current in a coil, and reduces with distance from the current source.

Designers should therefore place high current tracks and coils as far away as possible from the magnetometer. Ferromagnetic cores within coils become magnetized by both the coil current and the geomagnetic field creating additional soft iron interference.

An estimate of the magnetic field sourced by a PCB power supply track can be obtained from MAG3110's equation relating the curl of the magnetic field $\boldsymbol{B}$ to the local current density $\boldsymbol{j}$ and the time derivative of the local electric field $\boldsymbol{E}$:

$$\nabla \times \boldsymbol{B} = \mu_0 \boldsymbol{j} + \varepsilon_0 \mu_0 \frac{\partial \boldsymbol{E}}{\partial t} \qquad \textbf{Eqn. 1}$$

μ_0 is the permeability of free space and is defined to have value:

$$\mu_0 = 4\pi \times 10^{-7} \mathrm{NA}^{-2} \qquad \textbf{Eqn. 2}$$

If the PCB trace is straight with extent in both directions greater than the separation of the magnetometer from the trace, then edge effects can be ignored and the magnetic field will be rotationally symmetrical. With the additional constraint that the electric and magnetic fields are constant, Equation 1 can be rewritten using Stokes' theorem in terms of line and surface integrals for a closed circular path at normal distance $\boldsymbol{r}_0$ from the trace:

$$\oint_r \boldsymbol{B}.d\boldsymbol{r} = 2\pi r_0 B(r_0) = \iint_s (\nabla \times \boldsymbol{B}).d\boldsymbol{S} = \iint_s \mu_0 \boldsymbol{j}.d\boldsymbol{S} \qquad \textbf{Eqn. 3}$$

The current density $\boldsymbol{j}$ includes both free currents in the trace and bound currents in ferromagnetic materials. If there are no ferromagnetic materials in the vicinity of the magnetometer and PCB trace then the surface integral of the current density $\boldsymbol{j}$ simply equals the PCB trace current I. The return current flow through the ground plane is assumed to be spatially diffused and is ignored.

If, in addition, the less than one part in 10^6 difference in the magnetic permeability of air and vacuum is ignored in Equation 3, then the magnetic field $B(r_0)$ at distance r_0 from the PCB trace is given in Teslas by:

$$B(r_0) = \frac{\mu_0 I}{2\pi r_0} = \frac{0.2 \times 10^{-6} I}{r_0} \quad \textbf{\textit{Eqn. 4}}$$

Modern smartphone power traces can easily source 1A in current. At 10^{-3}m separation, the magnetic field from a 1A current trace will be 200 µT reducing to 20 µT at 10^{-2}m separation. This field will in turn induce a soft iron field in local ferromagnetic components on the PCB which may amplify the prediction of Equation 4 several times over.

The effects of time varying currents depend on their frequency. The highest sampling rate of a consumer magnetometer is approximately 100 Hz so currents at significantly higher frequencies will not be detectable by the magnetometer. Signals at lower frequencies may be detectable as modulation of the magnetic output and the compass heading. Incremental changes in current will create corresponding changes in the magnetic field and compass error.

The most difficult situation for the calibration software is the placement too close to the magnetometer of a power supply trace supplying a varying current depending on the smartphone processor load, the state of the LCD backlight and whether the RF power amplifier is active.

7 Other Sources of PCB Interference

PCB designers should also make industrial designers and mechanical engineers aware of the consequences of including magnetic materials into the smartphone housing. These should generally be avoided since they add to the overall hard and soft iron field. Industrial designers should be aware that different phone configurations (such as a clamshell phone being open or closed) also create different magnetic interference which further complicates the task of the calibration software.

NOTE:

Engineers should not attempt to shield the magnetometer from PCB hard iron or soft iron interference by placing the magnetometer or the interfering magnetic materials under shielding. Aluminum shielding is transparent to magnetic fields and has no effect. Steel shielding acts as an additional source of soft iron interference distorting both the direction and magnitude of the geomagnetic field and amplifying the effects of permanently magnetized components on the PCB.

8 Component and Material Selection

Components using iron, cobalt, nickel and their alloys (generally referred to as ferromagnets) can maintain a permanent magnetic field and are the predominant source of hard iron interference. Typical components with permanent magnetization include speaker magnets, vibrator and camera modules.

The same ferromagnetic materials when normally unmagnetized are responsible for the soft iron magnetic interference. Any external field, whether the hard iron or the geomagnetic field, induces a temporary magnetic field in these materials. Common sources of soft iron distortion include the smartphone battery and steel shields in the RF module.

Materials that are safe for use in the proximity of the magnetometer include brass, aluminum, copper, gold, silver and titanium.

The ability of a material to develop an induced soft iron field in response to an external field is proportional to its relative magnetic permeability μ_r. The relative permeabilities of common materials are shown in Table 1. Those with high relative permeabilities should be avoided wherever possible.

Table 1. Common Materials

Material	Relative Permeability μ_r
Mu-metal (75% Ni, 15% Fe, Cu, Mb)	25,000 and higher
Permalloy (80% Ni, 20% Fe)	8000
Iron (99.8% pure)	5000
Ferrite N41	3000
Ferrite M33	750
Nickel (99% pure)	600
Cobalt (99% pure)	250
Steel	100
Ferrite U60	8
Platinum	1.000265
Titanium	1.00005
Aluminum	1.000022
Brass	≈1.00000
Copper	0.999994
Silver	0.999974
Gold	0.99996

9 Experimental Determination of the Magnetometer Measurement Locus

In the complete absence of hard and soft iron interference (including any sensor offset), a magnetometer will accurately measure the three components of the geomagnetic field in the magnetometer frame of reference. Irrespective of the magnetometer orientation, the vector magnitude of the measured field will equal the magnitude of the geomagnetic field. At a different orientation, individual geomagnetic field components will be different but the vector magnitude will not change. Under arbitrary rotation, the locus of the magnetometer measurements will lie on the surface of a sphere centered at zero field with radius equal to the geomagnetic field magnitude.

The addition of a hard iron field adds a fixed vector offset to all measurements and displaces the locus of measurement by an amount equal to the hard iron offset. The measurement sphere is now centered at the hard iron offset but still has radius equal to the geomagnetic field strength.

Soft iron effects distort the measurement sphere along preferred axes and with differing gains along each axis. The measurement locus then becomes an ellipsoid centered at the hard iron offset and provides valuable information to the PCB designer on hard and soft iron distortions. The ellipsoid need not be aligned with the axes of the magnetometer.

The examples in the remainder of this section demonstrate the use of the Freescale RD4247MAG3110 eCompass evaluation PCB to obtain the ellipsoidal measurement locus. The RD4247MAG3110 eCompass PCB uses the Freescale MMA8451 accelerometer and MAG3110 magnetometer. The eCompass and calibration software executes from any PC and provides the facility to measure and record to disc a file containing magnetometer measurements made at differing roll, pitch and yaw angles.

User steps:

1. Place the magnetometer in the proposed location of the actual PCB magnetometer with the PCB's ferromagnetic components in their correct relative locations.
2. Run the RD4247MAG3110 PC software.
3. Gather magnetic measurements while orienting the assembly in differing directions.
4. Use the 'Save' button to write the measurements to an ASCII tab-delimited file to the PC disc drive.

Figure 3 shows the x-y, y-z and z-x slices through a measurement ellipsoid recorded by the RD4247MAG3110 in an environment of strong hard iron and soft iron interference.

In the figures, it is immediately apparent that:

- the hard iron offsets in the x, y, and z axes are approximately 150 μT, 30 μT and -150 μT.
- the measurement ellipsoid is significantly non-spherical and is not aligned with the measurement axes. There is therefore a strong soft iron effect with its highest permeability axis lying in the x-y plane and rotated some 30 degrees from the x-axis
- the measurements do not exceed the magnetometer measurement range and there is no clipping.

The levels of hard iron disturbance in these measurements are acceptable but the designer should probably not be happy with the level of soft iron interference. The Freescale calibration software is, however, quite capable of estimating and removing this strong soft iron distortion as demonstrated in Figure 6.

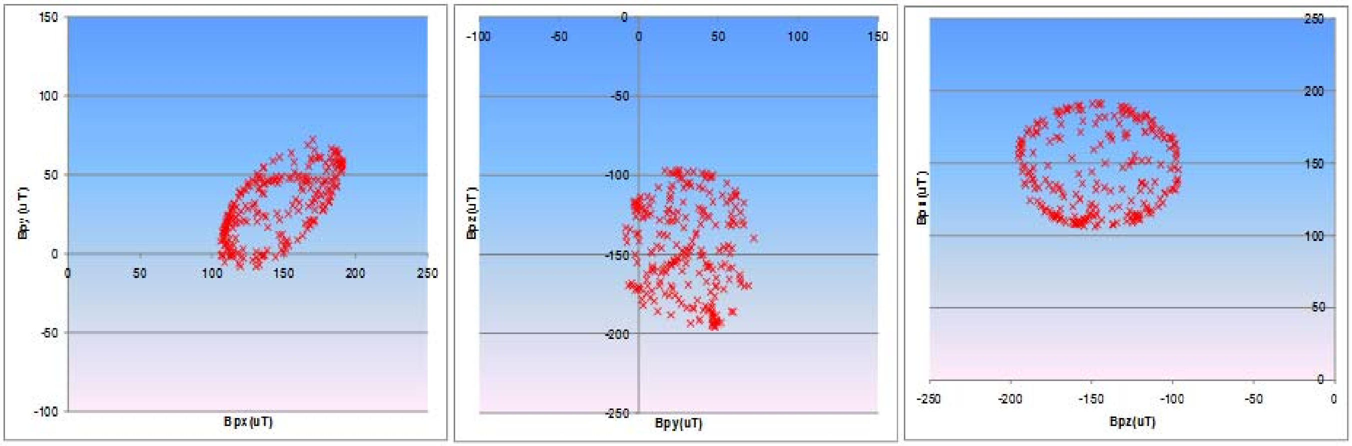

Figure 3. Measured magnetometer locus - no correction applied

Figure 4 shows a screen shot of the calibration coefficients computed by the RD4247MAG3110. The calculated hard iron offset provides a more accurate estimate than that provided by visual inspection of the scatter plot. The calculated inverse soft iron matrix has, as expected, significant off-diagonal terms in order to invert the strong soft iron disturbance on the measurements.

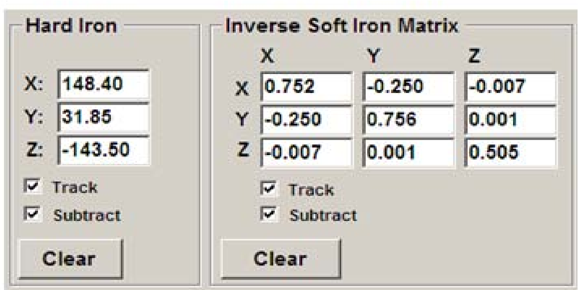

Figure 4. Calibration coefficients computed by the RD4247MAG3110 software

Figure 5 shows the measurement locus after correcting for the estimated hard iron offset. The data is now centered at the origin but still highly distorted by soft iron effects. The computed compass heading will not be accurate after applying hard iron corrections only.

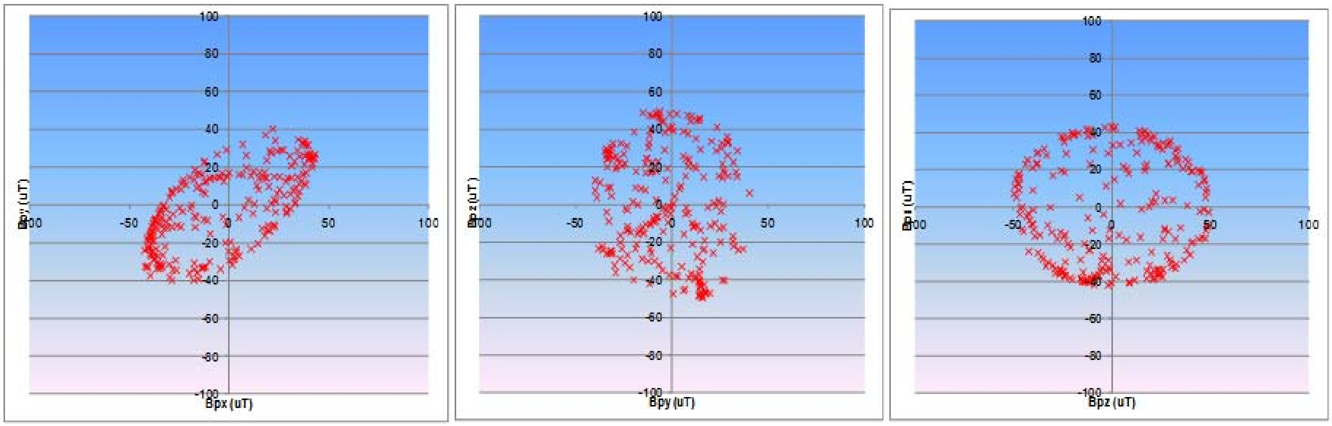

Figure 5. Measured magnetometer locus - hard iron correction applied

Figure 6 shows the measurement locus after applying the inverse soft iron matrix computed by the Freescale calibration algorithms (see Figure 4). The measurement locus is now a sphere centered at the origin with magnitude 25 µT and represents the locus of the geomagnetic field in the absence of hard and soft iron interference. Compass heading estimation using these measurements will be highly accurate.

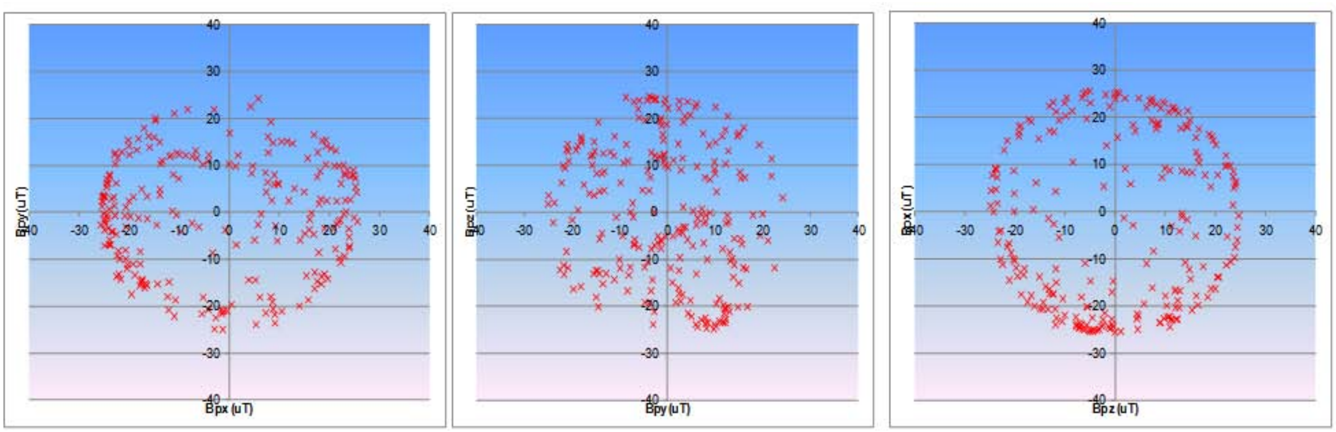

Figure 6. Measured magnetometer locus - hard and soft iron correction applied

10 Mathematical Annex

This section uses the same mathematical framework used in Application Note AN4248 "Implementing a Tilt-Compensated eCompass using Accelerometer and Magnetometer Sensors". It is recommended that AN4248 is read before this section.

The geomagnetic field vector $\boldsymbol{B}_r$, measured in the earth coordinate frame defined in AN4248, has magnitude B and inclination angle δ from horizontal:

$$\boldsymbol{B}_r = B\begin{pmatrix} \cos\delta \\ 0 \\ \sin\delta \end{pmatrix} \qquad \textbf{Eqn. 5}$$

The smartphone magnetometer $\boldsymbol{B}_p$ will measure the geomagnetic field after application of rotation matrices $\boldsymbol{R}_x(\phi)$, $\boldsymbol{R}_y(\theta)$, $\boldsymbol{R}_z(\psi)$ in roll, pitch and yaw, multiplication by the matrix $\boldsymbol{W}$ representing the soft iron distortion, and the addition of the hard iron offset vector $\boldsymbol{V}$:

$$\boldsymbol{B}_p = \boldsymbol{W}\boldsymbol{R}_x(\phi)\boldsymbol{R}_y(\theta)\boldsymbol{R}_z(\psi)\boldsymbol{B}_r + \boldsymbol{V} = \boldsymbol{W}\boldsymbol{R}_x(\phi)\boldsymbol{R}_y(\theta)\boldsymbol{R}_z(\psi)B\begin{pmatrix} \cos\delta \\ 0 \\ \sin\delta \end{pmatrix} + \boldsymbol{V} \qquad \textbf{Eqn. 6}$$

The locus of the geomagnetic field vector measured under arbitrary smartphone rotation in the complete absence of hard and soft iron effects, can be computed from its modulus squared as:

$$\boldsymbol{B}_p^T\boldsymbol{B}_p = \left\{\boldsymbol{R}_x(\phi)\boldsymbol{R}_y(\theta)\boldsymbol{R}_z(\psi)B\begin{pmatrix} \cos\delta \\ 0 \\ \sin\delta \end{pmatrix}\right\}^T\left\{\boldsymbol{R}_x(\phi)\boldsymbol{R}_y(\theta)\boldsymbol{R}_z(\psi)B\begin{pmatrix} \cos\delta \\ 0 \\ \sin\delta \end{pmatrix}\right\} \qquad \textbf{Eqn. 7}$$

$$= B^2\begin{pmatrix} \cos\delta \\ 0 \\ \sin\delta \end{pmatrix}^T\{\boldsymbol{R}_z(\psi)\}^T\{\boldsymbol{R}_y(\theta)\}^T\{\boldsymbol{R}_x(\phi)\}^T\boldsymbol{R}_x(\phi)\boldsymbol{R}_y(\theta)\boldsymbol{R}_z(\psi)\begin{pmatrix} \cos\delta \\ 0 \\ \sin\delta \end{pmatrix} = B^2 \qquad \textbf{Eqn. 8}$$

The modulus squared of the measurements equals the square of the geomagnetic field strength and the measurements lie on the surface of a sphere with radius B.

The locus of the magnetometer readings $\boldsymbol{B}_p$ under arbitrary rotations, but with hard and soft iron effects present, can be determined from Equation 6 as:

$$\{\boldsymbol{W}^{-1}(\boldsymbol{B}_p - \boldsymbol{V})\}^T\boldsymbol{W}^{-1}(\boldsymbol{B}_p - \boldsymbol{V}) = (\boldsymbol{B}_p - \boldsymbol{V})^T(\boldsymbol{W}^{-1})^T\boldsymbol{W}^{-1}(\boldsymbol{B}_p - \boldsymbol{V}) \qquad \textbf{Eqn. 9}$$

$$= B^2\left\{\boldsymbol{R}_x(\phi)\boldsymbol{R}_y(\theta)\boldsymbol{R}_z(\psi)\begin{pmatrix} \cos\delta \\ 0 \\ \sin\delta \end{pmatrix}\right\}^T\left\{\boldsymbol{R}_x(\phi)\boldsymbol{R}_y(\theta)\boldsymbol{R}_z(\psi)\begin{pmatrix} \cos\delta \\ 0 \\ \sin\delta \end{pmatrix}\right\} \qquad \textbf{Eqn. 10}$$

Using Equation 7, this simplifies to:

$$(\boldsymbol{B}_p - \boldsymbol{V})^T (\boldsymbol{W}^{-1})^T \boldsymbol{W}^{-1} (\boldsymbol{B}_p - \boldsymbol{V}) = B^2 \qquad \textbf{\textit{Eqn. 11}}$$

The general expression for the surface on an ellipsoid with coordinate vector ***R*** centered at $\boldsymbol{R}_0$ is (where ***A*** is a symmetric matrix):

$$(\boldsymbol{R} - \boldsymbol{R}_0)^T \boldsymbol{A} (\boldsymbol{R} - \boldsymbol{R}_0) = const \qquad \textbf{\textit{Eqn. 12}}$$

It can be readily proved that the product matrix $(\boldsymbol{W}^{-1})^T \boldsymbol{W}^{-1}$ is always symmetric. Equation 11 and 12 are therefore identical and show that the locus of magnetometer measurements $\boldsymbol{B}_p$ lies on the surface of an ellipsoid centered at the hard iron offset ***V*** with shape given by the soft iron matrix ***W***.

How to Reach Us:

Home Page:
www.freescale.com

Web Support:
http://www.freescale.com/support

USA/Europe or Locations Not Listed:
Freescale Semiconductor, Inc.
Technical Information Center, EL516
2100 East Elliot Road
Tempe, Arizona 85284
1-800-521-6274 or +1-480-768-2130
www.freescale.com/support

Europe, Middle East, and Africa:
Freescale Halbleiter Deutschland GmbH
Technical Information Center
Schatzbogen 7
81829 Muenchen, Germany
+44 1296 380 456 (English)
+46 8 52200080 (English)
+49 89 92103 559 (German)
+33 1 69 35 48 48 (French)
www.freescale.com/support

Japan:
Freescale Semiconductor Japan Ltd.
Headquarters
ARCO Tower 15F
1-8-1, Shimo-Meguro, Meguro-ku,
Tokyo 153-0064
Japan
0120 191014 or +81 3 5437 9125
support.japan@freescale.com

Asia/Pacific:
Freescale Semiconductor China Ltd.
Exchange Building 23F
No. 118 Jianguo Road
Chaoyang District
Beijing 100022
China
+86 10 5879 8000
support.asia@freescale.com

For Literature Requests Only:
Freescale Semiconductor Literature Distribution Center
1-800-441-2447 or +1-303-675-2140
Fax: +1-303-675-2150
LDCForFreescaleSemiconductor@hibbertgroup.com

Document Number: AN4247
Rev. 2
07/2011

freescale™ semiconductor